Accepted Manuscript

A systematically comparative study on $LiNO_3$ and Li_2SO_4 aqueous electrolytes for electrochemical double-layer capacitors

Jianbo Jiang, Beibei Liu, Guiyu Liu, Dong Qian, Chunming Yang, Junhua Li

PII: S0013-4686(18)30853-3

DOI: 10.1016/j.electacta.2018.04.097

Reference: EA 31664

To appear in: *Electrochimica Acta*

Received Date: 3 October 2017

Revised Date: 20 March 2018

Accepted Date: 13 April 2018

Please cite this article as: J. Jiang, B. Liu, G. Liu, D. Qian, C. Yang, J. Li, A systematically comparative study on $LiNO_3$ and Li_2SO_4 aqueous electrolytes for electrochemical double-layer capacitors, *Electrochimica Acta* (2018), doi: 10.1016/j.electacta.2018.04.097.

Graphical Abstract

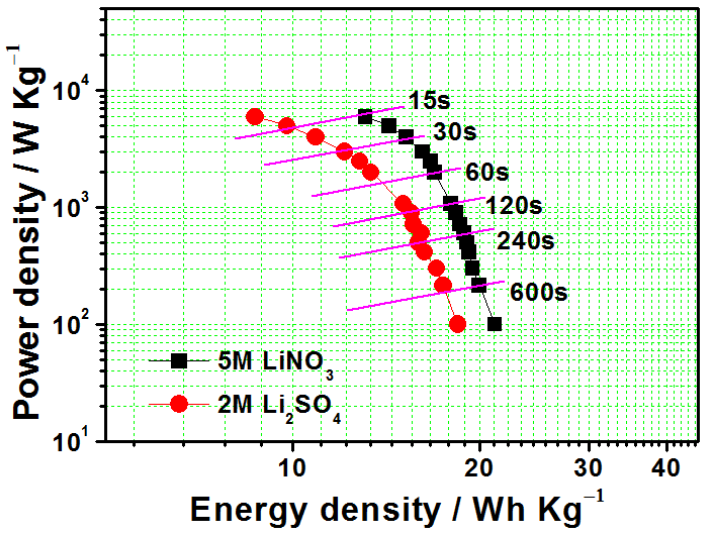

A systematically comparative study on $LiNO_3$ and Li_2SO_4 aqueous electrolytes for electrochemical double-layer capacitors

Jianbo Jiang [a,b], Beibei Liu [a], Guiyu Liu [a], Dong Qian [a,d,*], Chunming Yang [e], Junhua Li [c,**]

[a] Hunan Provincial Key Laboratory of Chemical Power Resources, College of Chemistry and Chemical Engineering, Central South University, Changsha 410083, PR China

[b] College of Chemistry and Chemical Engineering, Jishou University, Jishou 416000, PR China

[c] Key Laboratory of Functional Metal-Organic Compounds of Hunan Province, College of Chemistry and Material Science, Hengyang Normal University, Hengyang 421008, PR China

[d] State Key Laboratory of Powder Metallurgy, Central South University, Changsha 410083, PR China

[e] College of Chemistry and Chemical Engineering, Hunan Normal University, Changsha 410081, PR China

[*] Corresponding author. Tel/Fax: +86 731 88879616. E-mail address: qiandong6@vip.sina.com (D. Qian).

[**] Corresponding author. Tel/Fax: +86 734 8486779. E-mail address: junhua325@126.com (J. Li).

ABSTRACT

In this work, highly soluble $LiNO_3$ was adopted as the neutrally aqueous electrolyte for active carbon (AC)-based electrochemical double-layer capacitors (EDLCs), of which the electrochemical performances were evaluated. Simultaneously, the physicochemical properties such as the ionic conductivity and viscosity of the $LiNO_3$ aqueous solution were investigated. As compared with the most studied Li_2SO_4 aqueous solution, the $LiNO_3$ aqueous solution displays more favorable physicochemical properties and electrochemical performances as the neutral electrolytes for EDLCs. To be specific, the conductivity of the 5.0 M $LiNO_3$ aqueous solution can reach up to 154.8 mS cm^{-1} at 25 °C, which is nearly two times of the maximum conductivity of 77.6 mS cm^{-1} for the 2.0 M Li_2SO_4 aqueous solution under the identical testing conditions. Even at a concentration as high as 9.0 M, the absolute viscosity of the $LiNO_3$ aqueous solution is only 2.4, while that of the Li_2SO_4 aqueous solution achieves 3.0 at the maximum concentration of 2.5 M. Additionally, 5.0 M $LiNO_3$ aqueous solution exhibits a wide electrochemical potential stability window from −0.9 to 0.9 V (vs. SCE) at the AC electrode, giving rise to an operating cell voltage of 1.8 V, which is comparable to that of 2.0 M Li_2SO_4 aqueous solution. Further, with the 5.0 M $LiNO_3$ aqueous solution as the electrolyte, the as-fabricated EDLC delivers an energy density up to 21.16 Wh Kg^{-1} at a power density of 100.09 W kg^{-1}, which is higher than 18.43 Wh Kg^{-1} for the EDLC with the 2.0 M Li_2SO_4 aqueous electrolyte at the identical power density. Even though the power density reaches as high as 5970 W Kg^{-1}, the energy density of the EDLC with the 5.0 M $LiNO_3$ aqueous electrolyte can still remain at 13.1 Wh Kg^{-1}, substantially higher than 8.71 Wh Kg^{-1} of the EDLC with the 2.0 M Li_2SO_4 aqueous electrolyte at the same power density. Moreover, the EDLC with the 5.0 M $LiNO_3$ aqueous electrolyte also

holds good cyclic stability. After 10000 charge–discharge cycles at a current density of 1 A g^{-1} and a cut-off voltage of 1.8 V, the capacity retention of this EDLC retains more than 90%. These results can render an insight to explore safe, eco-friendly, inexpensive and neutrally aqueous electrolytes for supercapacitors.

Keywords: $LiNO_3$ aqueous electrolyte; Li_2SO_4 aqueous electrolyte; Conductivity; Viscosity; Supercapacitive performance

1. Introduction

With the increasing fossil fuel depletion and environment deterioration arising from the excessive utilizations of fossil fuels, exploring green, renewable and sustainable energy becomes the top priority. On this way, electrochemical energy storage and conversion devices including lithium ion batteries (LIBs) and electrochemical capacitors (ECs) have attracted intense attention [1−4].

ECs are considered as promising energy storage and conversion devices due to their merits on the high power output and long cycle life [5,6]. These advantages make ECs be complementary devices for LIBs and power the new energy vehicles [7]. Moreover, ECs can also act as the frequency-regulating devices in the large smart grids [8]. Undoubtedly, these applications of ECs are of great significance in promoting the development of green and sustainable energy.

On the basis of the charge storage mechanism, ECs are often categorized as electrochemical double-layer capacitors (EDLCs) and pseudocapacitors [9]. Although the pseudocapacitors based on the faradic interfacial reaction can provide high specific energy, the symmetric EDLCs still remain superior because of the high power, long cycling stability and calendar life [10].

The electrolytes, important components for EDLCs, play a fundamental role in the electric double-layer formation and are one of the decisive factors for the EDLC performances [11]. In general, the electrolytes applied in EDLCs are principally aqueous electrolytes, organic electrolytes and ionic liquids [12]. In all conscience, these electrolytes have their own advantages and disadvantages.

Up to now, the most frequently utilized electrolytes in EDLCs are organic media owing to the allowed operating voltages, and the resulting higher energy densities of EDLCs [13]. However, these have to be balanced with some drawbacks, such as being

flammable, expensive and hazardous to the environment.

Ionic liquids have been proposed as the environmentally friendly and safe electrolytes for EDLCs, and enable the devices to operate at voltages of as high as 3.5–3.7 V accompanied with high cycling stability [14,15]. However, because of the relatively high viscosity and low conductivity, the equivalent series resistance (ESR) values of ionic liquids-based EDLCs at room temperature are frequently higher than those of conventional electrolytes [16]. Moreover, the high cost also hinders their applications as electrolytes.

In comparison with the organic media, the main shortcoming of EDLCs employing acidic and basic aqueous electrolytes lies in the much lower electrochemical windows [17]. For example, with respect to the organic electrolytes, the operating voltage of EDLC can attain ca. 2.7 V [18] but only around 1.0 V for H_2SO_4 and KOH electrolytes (thermodynamically limited stability window of water at 1.23 V) [19,20]. However, aqueous solutions can afford higher ionic conductivity, lower ESR and better safety than the organic ones, and the purifications and highly expensive drying processes are not required [21]. Therefore, it is of cardinal significance to search for proper aqueous electrolytes which can increase the operating voltages of EDLCs.

Recently, neutral alkaline metal sulphate aqueous solutions such as Na_2SO_4 [22−24], Li_2SO_4 [25−28] and K_2SO_4 [29] as electrolytes for ECs have received considerable popularity owing to the electrochemical stability, wide electrochemical stability potential window (ESPW), non-corrosiveness and environmental friendliness. In particular, the wide ESPW of ~1.9 V for these aqueous sulphate salts (due to the shift of the potentials for H_2 evolution at the cathode electrode to lower values) opens up the possibility of employing these fascinating aqueous electrolytes without significantly compromising on the energy densities of the EDLCs [25,27,29].

However, most of the alkaline metal sulphates suffer from the low solubilities, for example, 16.3 g/100 mL (1.32 M) for Na_2SO_4 and 11.1 g/100 mL (0.64 M) for K_2SO_4 at 20 °C [30], which will give the low ionic conductivities of their aqueous solutions.

More recently, Luo et al. [31] reported the microporous carbon for supercapacitors with a $LiNO_3$ neutrally aqueous electrolyte, in which they just investigated the effect of different concentrations of $LiNO_3$ electrolytes on the electrochemical performances of supercapacitors. To further cast new light on the safe, cheap and environmentally benign $LiNO_3$ electrolyte, a detailed and systematical study on this electrolyte is important and necessary, especially an indispensable comprehensive comparison with the most studied analog Li_2SO_4. By contrast, we have noticed that $LiNO_3$ possesses much higher solubility with 70.1 g/100 mL (10.17 M) than that of $Li_2SO_4 \cdot H_2O$ with 34.8 g/100 mL (2.72 M) at 20 °C [30], which is the highest solubility value among the alkaline sulphates. Due to the high solubility of $LiNO_3$, people can reasonably expect good performances of EDLCs using the aqueous $LiNO_3$ solution as the electrolyte over the Li_2SO_4 aqueous solution.

In the present work, we report the electrochemical performances of the active carbon (AC)-based EDLCs with the $LiNO_3$ aqueous electrolytes characterized by cyclic voltammetry (CV), galvanostatic charge–discharge (GCD) and electrochemical impedance spectrum (EIS) systematically, and the physicochemical properties of the $LiNO_3$ aqueous solution such as the ionic conductivity and viscosity. As compared with the Li_2SO_4 aqueous solution, the $LiNO_3$ aqueous solution displays more favorable physicochemical properties and electrochemical performances as the neutral electrolytes for EDLCs. To our best knowledge, the comparison of the $LiNO_3$ aqueous electrolyte with the Li_2SO_4 aqueous electrolyte for EDLCs was reported for the first time.

2. Experimental

2.1. Preparations of aqueous electrolytes

$LiNO_3$ and $Li_2SO_4·H_2O$ were of analytical grade and purchased from Aladdin Chemistry Co., Ltd. (Shanghai, China). The ultrapure water (18.3 MΩ cm) was obtained utilizing a Milli-Q water system and used throughout the experiments. The $LiNO_3$ aqueous solutions with concentrations of 0.01, 0.1, 1.0, 2.0, 3.0, 4.0, 5.0, 6.0, 7.0, 8.0 and 9.0 M as well as the Li_2SO_4 aqueous solutions with concentrations of 0.01, 0.1, 0.5, 1.0, 2.0, 2.2 and 2.5 M were accurately prepared in a 250 mL volumetric flask. It should be noted that the maximum concentration of the Li_2SO_4 aqueous solution was limited to be 2.5 M at 25 °C due to the low solubility of $Li_2SO_4·H_2O$.

2.2. Conductivity and viscosity measurements

A high conductivity meter (MP515-03, Shanghai San-Xin Instrumentation, Inc., China) with a 2401-M glass conductivity electrode (cell constant K = 1.0 cm^{-1}) was adopted to determine the conductivities of the as-prepared aqueous electrolytes. Prior to the determinations of conductivities, the conductivities of KCl solutions in the concentration range of 0.001−1.0 M at 25 °C were used for the calibration. During the measuring process, the fiducial temperature was set at 25 °C, and the minimum volume of the solution was 10 mL to ensure the complete immersion of the conductivity electrode.

The ionic viscosity measurements of the $LiNO_3$ and Li_2SO_4 aqueous solutions were conducted using an Ubbelohde viscometer according to the literatures [32,33], and the relative viscosities to the pure water were obtained. The time that the liquid (water or solution) flowed through the glass ball of the Ubbelohde viscometer was measured three times for each sample. The deviation was controlled to be less than 0.3 s, and the average value was taken to calculate the relative viscosity**.** The absolute viscosity

η was derived from the relative viscosity according to the following equation [34]:

$$\eta = 0.8903\eta_r \qquad (1)$$

where η_r is the relative viscosity of a sample solution, 0.8903 is the viscosity of pure water at 25 °C.

2.3. Preparation of electrode and electrochemical tests

Porous AC powders (YEC-8A) purchased from Fuzhou Yihuan Carbon Co., Ltd. , (Fuzhou, China) was used as the electro-active material. The detailed specifications, morphology and pore properties of the AC powders can be found in Supporting Information (SI). The 316L stainless steel mesh was appointed as the current collector. Two kinds of working electrodes were fabricated. The first electrode with 1 cm^2 sectional area and 9−10 mg electro-active material was rectangular-shaped, and used for the single electrode test. The second electrode with 2.25 cm^2 sectional area and 15−20 mg electro-active material was disk-shaped, and used for the complete cell measurement. The AC electrode was prepared by pressing a mixture of AC, acetylene black and poly(tetrafluoroethylene) (PTFE) in a weight ratio of 85:10:5 onto the 316L stainless steel mesh, and the method for preparing this kind of electrode could be found elsewhere [35,36].

EIS measurements were conducted on a CHI760D electrochemical station (Shanghai Chenghua Instrument Co. Ltd, China). The GCD cycle tests of complete cells were performed on a CT-4008 battery testing system with a 7.5x soft system (Neware Technology Co. Ltd, China). For the single electrode test, a saturated calomel electrode (SCE) and a platinum gauze were used as the reference and counter electrodes, respectively. An H-type glass cell with membranes was employed to avoid the effect of over polarization on the electrode potential due to O_2 and H_2 evolutions during testing. For the complete cell test, a special assembly was fabricated according

to the literature [37]. All measurements were performed at room temperature.

3. Results and discussion

3.1. Conductivity and viscosity measurements

The conductivity and viscosity are fundamental physical properties of a solution. However, for the EDLC applications, these two properties are of technical importance. This is because that the electrolytic conductivity directly affects the ESR of a capacitor, and generally the higher ESR causes a higher energy loss during the charge−discharge cycles. On the other hand, as to the electrolytic salt solutions, the higher viscosities usually result in lower conductivities [38]. However, a high conductivity as well as a low viscosity of an electrolyte is essential prerequisites for a high-performance EDLC.

The conductivity and relative viscosity values obtained at 25 °C for all the considered electrolytes are given in Fig. 1. From Fig. 1, it can be seen that both the $LiNO_3$ and Li_2SO_4 aqueous solutions exhibit higher conductivities with 10−160 mS cm^{-1} than those of most organic liquid electrolytes with 1.7−50 mS cm^{-1} [39−42]. They also show much lower dynamic viscosity values with 1−2.5 mPa s (calculated on the basis of 0.8903 mPa s for the pure water [34,43]) than those of most ionic liquids with 30−600 mPa s [40], indicating that the aqueous electrolytes hold more desirable conductivities and viscosities over organic electrolytes.

Fig. 1.

It can be also obviously observed from Fig. 1 that the $LiNO_3$ aqueous solutions have higher ionic conductivities than the Li_2SO_4 aqueous solutions, except the close values at low concentrations (0.01−0.1 M). Both conductivity curves of the $LiNO_3$ and Li_2SO_4 aqueous solutions show hump-shaped profiles, confirming the existence of inflection points. For the Li_2SO_4 aqueous solution, the maximum conductivity

value of 77.6 mS cm^{-1} appears at 2.0 M. Surprisingly, for the $LiNO_3$ aqueous solution, the maximum conductivity value reaches up to 154.8 mS cm^{-1} at 5.0 M, which is nearly two times of that for the Li_2SO_4 aqueous solution.

From Fig. 1, it is as well evidently found that the $LiNO_3$ aqueous solutions possess lower viscosities than the Li_2SO_4 aqueous solutions. For example, even at a concentration of as high as 9.0 M, the absolute viscosity of the $LiNO_3$ aqueous solution is only 2.4, while that of the Li_2SO_4 aqueous solution achieves 3.0 at the maximum concentration of 2.5 M. Additionally, the viscosity profile of the Li_2SO_4 aqueous solution exhibits a much more steep slop than that of the $LiNO_3$ aqueous solution upon increasing the concentration, corroborating a more rapid increase of the viscosity for the Li_2SO_4 aqueous solution with raising the concentration. When the concentration of the $LiNO_3$ aqueous solution rises from 0.01 to 9.0 M, the absolute viscosity increases from 0.9 to 2.4. The increment is only 1.5, while an increment of 2.1 is found for the Li_2SO_4 aqueous solution when its concentration varies from 0.01 to 2.5 M.

The reason for the higher conductivity and lower viscosity of the $LiNO_3$ aqueous solution as compared with the Li_2SO_4 aqueous solution is in connection with the fact that the hydrated NO_3^- possesses a smaller ion radius of 0.31 nm than that of 0.5 nm for the hydrated SO_4^{2-} [44]. The smaller the ion is, the faster ion moves. The high conductivity and low viscosity of the $LiNO_3$ aqueous electrolyte will undoubtedly favor the enhancement of electrochemical performances for EDLCs.

3.2. EIS analysis

EIS measurements have been carried out in order to further investigate the ionic conductive effects of the 5 M $LiNO_3$ and 2 M Li_2SO_4 aqueous solutions with the optimum conductivities on the internal resistances of actual EDLCs. Two AC-based

EDLC cells with the 5.0 M $LiNO_3$ and 2.0 M Li_2SO_4 aqueous electrolytes were fabricated, and the EIS measurements were performed in a frequency range of 100 kHz−0.01 Hz with an amplitude of 5 mV. The EIS testing results given as Nyquist plots are depicted in Fig. 2.

Fig. 2.

Fig. 2(a) illustrates the Nyquist plots for the EDLC cells with the 5.0 M $LiNO_3$ and 2.0 M Li_2SO_4 aqueous electrolytes in 1:1 coordinates. From Fig. 2(a), it can be seen a semicircle following a spike appear in the high and low frequency ranges, suggesting the typical characteristic of EIS for the actual EDLCs [45−49].

To attain more useful information for the EIS analysis, the axis scales of Fig. 2(a) are enlarged and presented as Fig. 2(b). In Fig. 2(b), Nyquist plots are divided into two parts of equivalent series resistance (ESR) and equivalent distribution resistance (EDR). It can be seen that the difference of Nyquist plots between the two EDLC cells with the 5.0 M $LiNO_3$ and 2.0 M Li_2SO_4 aqueous electrolytes is noticeable. Firstly, the difference of ESR between these two EDLC cells highlights the advantage of the 5.0 M $LiNO_3$ aqueous electrolyte with high conductivity over the 2.0 M Li_2SO_4 aqueous electrolyte. Generally, the intercept of the curve with the real-axis in the high-frequency region (marked by the box in Fig. 2(b)) represents the ESR value, which commonly reflects the electronic resistance of the electrode and the ionic resistance of the bulk electrolyte [46,49]. As shown in Fig. 2(b), the ESR value of the EDLC cell with 5 M $LiNO_3$ (1.37 Ω) is lower than that of the EDLC cell with 2 M Li_2SO_4 (1.54 Ω). In this work, the electronic resistance of each electrode can be counted to be identical due to the same material composition in the electrode and no difference in the fabrications of EDLC cells. Therefore, the ESR value discrepancy between these two EDLC cells should mainly result from the ionic resistances of bulk

electrolytes.

Moreover, the EDR difference between these two EDLC cells further underscores the advantage on ion accessibility of the 5.0 M $LiNO_3$ aqueous electrolyte with high conductivity over the 2.0 M Li_2SO_4 aqueous electrolyte. In Fig. 2(b), the line segment that represents EDR for the 5.0 M $LiNO_3$ aqueous electrolyte is substantially less than that for the 2.0 M Li_2SO_4 aqueous electrolyte, indicating greater ion accessibility of the 5.0 M $LiNO_3$ aqueous electrolyte over the 2.0 M Li_2SO_4 aqueous electrolyte [49,50].

Furthermore, all the points marked by the circles in Fig. 2(c) are corresponding to a frequency value of 0.097 Hz, which is the upper frequency limit for the double-layer capacitance region ("knee" at low frequencies of $\leq$ 0.1 Hz) [51], and the extrapolated intercepts of the tangent lines passing through this limit point on the real-axis represent the total internal resistance values of the cells [52]. Hence, the total internal resistance values of the cells with the 5 M $LiNO_3$ and 2 M Li_2SO_4 aqueous electrolytes are 3.4 and 4.1 Ω, respectively, coinciding with the order of their ESR values. These results highlight again the advantage of high conductivity for the electrolyte.

Fig. 3.

The comparisons of series capacitance (Cs) vs. the logarithm of frequency (log(f)) and parallel capacitance (Cp) vs. log(f) plots at very low frequency has been made, and the results are shown in Fig. 3(a). The Cs and Cp values overlap at f < 0.09 Hz, indicating that almost blocking capacitive behaviors have been achieved for both electrodes at low AC frequency values [53].

In addition, the dependences of the logarithm of the absolute value of the imaginary impedance ($|-Z''|$) vs. log(f) have been plotted according to the Orazem et al.'s

model [54] (see Fig. 3(b)). It can be seen that the slope values are nearly −1, suggesting characteristic of ideally polarizable geometrically flat or very well blocked electrode [55]. As seen from Fig. 3, however, the systems under study cannot be used for high power density supercapacitors since the adsorption equilibrium can be established only at very limited cell potential region.

In order to further re-examine the dependence of capacitances of the cells with the 5 M $LiNO_3$ and 2 M Li_2SO_4 aqueous electrolytes on the frequencies, EIS data are transferred into the real mass specific capacitances (C_s') according to the following equation [52,56]:

$$C'_s = -\frac{Z''}{\omega |Z|^2 m} \qquad (2)$$

where ω = 2πf, m represents the total mass of activated materials on the basis of two electrodes of one cell, Z is the total impedance, and Z'' corresponds to the imaginary impedance. The results are presented in Fig. 4. Usually, the low-frequency value of C_s' for an EDLC corresponds to the static capacitance, which can be measured during the constant current discharge. It can be clearly seen from Fig. 3 that the cell with the 5 M $LiNO_3$ aqueous electrolyte holds the greater C_s' value than that with the 2 M Li_2SO_4 aqueous electrolyte. According to the equation $E = 0.5CU^2$, where E, C and U correspond to the energy, capacitance and operating voltage of a supercapacitor, respectively, it can be speculated that the cell with the 5 M $LiNO_3$ aqueous electrolyte will deliver the largest energy density at the same cut-off voltage.

Fig. 4.

Ordinarily, utilizable capacitance is determined by the ionic accessibility into the pores in the porous AC electrode [49], and the high C_s' of the cell with the 5 M $LiNO_3$ aqueous electrolyte reflects the favorable ionic accessibility of the 5 M $LiNO_3$

aqueous electrolyte, because the accessibility of electrolyte ions strongly depends on the radii of hydrated cations and anions in the aqueous solution.

3.3. ESPW determination

The ESPW is another important indicator for the performance evaluation of an electrolyte which is directly related to the operating cell voltage of an EDLC. Normally, a wider ESPW of an electrolyte can lead to a higher operating cell voltage for the EDLC using this electrolyte, and further bring about a larger energy output of the EDLC according to the equation $E = 0.5CU^2$. However, it should be pointed out that there does not exist a uniform standard so far for defining and measuring the ESPW of an electrolyte, though it is of importance for the electrolyte property assessment.

A conventional method to determine the ESPW of an electrolyte is based on the *i*−*V* polarization curve obtained by LSV or CV at an assigned current density with a nonporous inert electrode, e.g. Pt or glassy carbon electrode, as the working electrode [57]. The region between the two limits of oxidation and reduction potentials on the *i*−*V* polarization curve is ESPW. According to this method, we used a platinum sheet (1 cm^2) as the working electrode, and the LSV tests were performed for the 2.0 M Li_2SO_4 and 5.0 M $LiNO_3$ aqueous electrolytes at a scan rate of 5 mV s^{-1}, respectively, of which results are illustrated in Fig. 5. As can be seen from Fig. 5, the ESPW values for the 2.0 M Li_2SO_4 and 5.0 M $LiNO_3$ aqueous electrolytes are 2.0 and 2.1 V, respectively. Note that the ESPW for the $LiNO_3$ aqueous electrolyte is somewhat more positive than that for the Li_2SO_4 aqueous electrolyte, which is consistent with the result reported by Wessells et al. [58].

Fig. 5.

However, the ESPW obtained from the conventional method with the Pt or glassy carbon electrode as the working electrode is sometimes considered to be inaccurate and even misleading, since in a real device the working electrode is not the Pt or glassy carbon [59], and the electrochemical environments of electrolytes should not be neglected due to the fact that the faradic currents might be masked by the huge double-layer charging currents which occur at the electrode upon polarization [60].

For this reason, another approach called *R*-value method [60,61] was adopted to determine the ESPW for the 2.0 M Li_2SO_4 and 5.0 M $LiNO_3$ aqueous electrolytes. In this method, a dimensionless ratio *R* is utilized and defined as $R = |Q_F|/|Q_{NF}| = |Q_C|/|Q_D| - 1$, where *Q* is the charge quantity pass through the electrode, and *F*, *NF*, *C* and D represent faradic, non-faradic, charging and discharging, respectively. For a three-electrode system, $R = 0.1$ is set as the limit to determine the electrochemical window, which is achieved when the decomposition of electrolyte accounts for 10% non-faradic charge infused into the capacitor [59]. In terms of this method, the CV curves obtained at a scan rate of 5 mV s^{-1} and 25 °C with a 1 cm^2 AC electrode as the working electrode and 2.0 M Li_2SO_4 or 5.0 M $LiNO_3$ aqueous solution as the electrolyte are exhibited in Fig. 6(a and b), respectively. Correspondingly, the plots of evolution of the *R* factor vs. the vertex potential for the 2.0 M Li_2SO_4 and 5.0 M $LiNO_3$ aqueous electrolytes are given in Fig. 6(c), respectively.

Fig. 6.

As revealed from Fig. 6(c), in the negative half region (from −1.0 to 0 V) for the 2.0 M Li_2SO_4 aqueous electrolyte, all the *R* values to which the vertex potentials correspond are less than 0.1, even at the vertex potential of −1.0 V, indicating the

electrochemical stability of the electrolyte investigated in this region. In contrast, in the positive half region (0−1.0V), the *R* value is greater than 0.1 when the vertex potential exceeds 0.8 V, vindicating the decomposition of the electrolyte. Moreover, in this vertex potential region, it can be found a rapid increase of current as shown in Fig. 5(a). Accordingly, the ESPW for the 2.0 M Li_2SO_4 aqueous electrolyte is from −1.0 to 0.8 V determined by the *R*-value method, and hence an operating cell voltage of around 1.8 V can be attained for EDLCs using this electrolyte. Regarding the 5.0 M $LiNO_3$ aqueous electrolyte, the ESPW determined by the *R*-value method changes little to a range from −0.9 to 0.9 V. Nonetheless, an operating cell voltage of approximately 1.8 V is still available for EDLCs. Notably, the ESPW values obtained from the *R*-value method on the AC electrode is narrower than those from the conventional method on the Pt electrode. For the purpose of further affirming this situation, the GCD curves of AC-based EDLCs with the 2.0 M Li_2SO_4 and 5.0 M $LiNO_3$ aqueous electrolytes at 500 mA g^{-1} in a cell voltage rage of 1.2−2.0 V have been measured as provided in Fig. 7. From Fig. 7, it can be found that both the charge curves for these two solutions become curvature and off track when the cell voltage exceeds 1.8 V, while the charge curves in the range of 1.2−1.8 V are almost on the same line, which also verifies that the operating cell voltages of these two electrolytes can not break through 1.8 V.

Fig. 7.

Table 1

Additionally, for further establishing the realistic potential of the two electrode cell when the GCD curve is non–linear, a more precise method is employed by calculating the energy efficiencies within the fixed cell potentials after integrating the non–linear GCD data according to Laheäär et al.'s report [62]. Table 1 gives the energy efficiency

(η_E) together with columbic efficiency (η_t) values of cells with 2.0 M Li_2SO_4 and 5.0 M $LiNO_3$ aqueous electrolytes at 1.2, 1.4, 1.6, 1.8 and 2.0 V. In the cell potential range of 1.2−1.8 V, the η_E values decrease slowly for these two cells. With the cell potential exceeding 1.8 V, the η_E values drop dramatically, implying that the limit voltages for these two cells are 1.8 V during the charge processes, which conform to the results of the *R*-value method on the whole. Unfortunately, the data presented show that the materials and electrolytes under study are not the best for highly efficient supercapacitors characterized by high energy efficiency values, and hence the prototypes under study cannot be used for energy efficient systems.

3.4. Rate capability test

The rate capability, reflecting the charge−discharge capability at high current densities, is an important index to the performances of EDLCs. Thanks to the fact that the rate capability is closely correlated with either electrode materials or electrolytes of EDLCs, the serviceability of electrolytes for EDLCs at high current densities can be assessed via comparing the rate capabilities of EDLCs with the same electrode materials when employing these electrolytes.

The dependence of the capacitance for an EDLC on the current variation can be reflected by the CV technique, and thus it is the most popular method to evaluate the rate capability of an EDLC. Herein, the rate capabilities of two EDLCs using respective 2.0 M Li_2SO_4 and 5.0 M $LiNO_3$ aqueous electrolytes have been evaluated by means of the CV technique with the current response expressed as the specific capacitance according to literatures [56,58,59], of which results are displayed in Fig. 8. As shown from Fig. 8, both the CV curves of EDLCs approach the typical rectangular shapes at low sweep rates, indicating exactly the capacitive behaviors. At 10 mV s^{-1}, the specific capacitance of the EDLC with the 2.0 M Li_2SO_4 aqueous electrolyte is

less than 40 F g^{-1}, while the specific capacitance of the EDLC with the 5.0 M $LiNO_3$ aqueous electrolyte is greater than 40 F g^{-1}, suggesting a bigger capacitance can be achieved for the 5.0 M $LiNO_3$ aqueous electrolyte. The better rate capability of the EDLC with the 5.0 M $LiNO_3$ aqueous electrolyte over the 2.0 M Li_2SO_4 aqueous electrolyte can be further testified from Fig. 9, in which the dependence of specific capacitance retentions of these two EDLCs on the sweep rates is given. It should be noted that for the systems with moderate series resistance, the correction of CV curves before calculating parameters should be used [63]. Since the CV curves at 500 mV s^{-1} are far away from the rectangle, and according to the literature [64], with the time constant τ < 0.5 s, the specific capacitances were calculated only in the sweep rate range of 10−200 mV s^{-1}. It can be seen that the specific capacitance retentions of the EDLC with the 5.0 M $LiNO_3$ aqueous electrolyte are distinctly greater than those with the 2.0 M Li_2SO_4 aqueous electrolyte in the sweep rate range of 50−200 mV s^{-1}.

Fig. 8.

Fig. 9.

3.5. Power density and energy density measurements

The power density and energy density are important performance metrics for all energy storage and conversion systems including EDLCs, which directly concern their end applications. By using the results of GCD cyclic tests (displayed in the following section of 3.6) in a current density range of 0.056−3.34 A g^{-1} with the cut-off voltage of 1.8 V, the average energy densities and average power densities for the cells with the 2.0 M Li_2SO_4 and 5.0 M $LiNO_3$ aqueous electrolytes are obtained and illustrated with Ragone-like plots in Fig. 10, and a series of discharge isotime lines from 15 to 600 s are presented as well. The power density (P) and energy density

(*E*) in Fig. 9 were obtained by measuring the discharge times at different current densities, and calculated according to the following equations (3–4) [18, 62]:

$$E = \int_{t1}^{t2} IVdt \qquad (3)$$

$$P = \frac{E}{t} \qquad (4)$$

where *I* represents the charge–discharge current, *t* refers to the discharge time, and V is the cell voltage.

As illustrated from Fig. 10, both the cells show good performances in terms of the specific energy and power, underscoring the advantages of neutral aqueous electrolytes for EDLCs. With the 2.0 M Li_2SO_4 aqueous electrolyte, the cell delivers an energy density up to 18.43 Wh kg^{-1} at a low power density of 100.09 W kg^{-1}, higher than 16.9 Wh kg^{-1} at 200 W kg^{-1} reported by Sun et al. [48]. Strikingly, with the substitution of the 2.0 M Li_2SO_4 aqueous electrolyte by the 5.0 M $LiNO_3$ aqueous electrolyte, the maximum energy density of the cell rises to 21.16 Wh kg^{-1} at the identical power density. Moreover, the cell with the 5.0 M $LiNO_3$ aqueous electrolyte can afford an energy density as high as 13.1 Wh kg^{-1} even at the power density 5970 W kg^{-1}, substantially higher than 8.71 Wh kg^{-1} at the same power density for the cell with the 2.0 M Li_2SO_4 aqueous electrolyte. As a group, the good performance in terms of specific energy and power for the cell with the 5.0 M $LiNO_3$ aqueous electrolyte is ascribed to its high ionic conductivity, low viscosity and high molarity, but in the final analysis, is owed to the high solubility of $LiNO_3$ salt. It has been sufficiently demonstrated that the fundamental property of the electrolyte salt plays a key role in the electrochemical performances of EDLCs.

Fig. 10.

3.6. Cycling stability evaluation

In order to further compare the electrochemical stabilities of the cells with the 2.0

M Li_2SO_4 and 5.0 M $LiNO_3$ aqueous electrolytes, the GCD cycling behaviors of these two cells were examined by a NEWARE battery tester, and the results are presented in Fig. 11. As confirmed from Fig. 10, both the cells exhibit good cycling stabilities. For the cell with the 5.0 M $LiNO_3$ aqueous electrolyte, 90.8% capacitance retention of the maximum specific capacitance can be maintained after 10000 cycles at a current density of 1 A g^{-1} and a cut-off voltage of 1.8 V, accompanied with the coulombic efficiency of more than 98% throughout the cycles. Notably, after 1000 cycles, the specific capacitance almost remains stable up to the 10000th cycle. Regarding the cell with the 2.0 M Li_2SO_4 aqueous electrolyte, 89.4% capacitance retention of the specific capacitance can be remained after 10000 cycles, and the coulombic efficiency is kept at ~99% during the entire cycles. As to the reason for the better capacitance retention of the cell with the 5 M $LiNO_3$ aqueous electrolyte than that with the 2.0 M Li_2SO_4 aqueous electrolyte, we think this is related to the Li_2SO_4 concentration decrease in the cell with the 2.0 M Li_2SO_4 aqueous electrolyte, because the crystal deposit phenomenon of Li_2SO_4 in this cell has been observed during long-time cycling. The higher specific capacitance for the 5 M $LiNO_3$ cell (~38 F g^{-1}) compared with the 2.0 M Li_2SO_4 cell (~30 F g^{-1}) can be ascribed to the smaller size of the monovalent NO_3^- ions in an electrosorbed nohydrated state as compared to the hydrated bivalent SO_4^{2-} ions [44,46,65]. Finally, the good cyclic stability of the cell using the $LiNO_3$ aqueous electrolyte attests once again that the uses of $LiNO_3$ aqueous electrolyte for EDLCs are not detrimental to the corresponding cycling abilities, as also pointed out by Brousse et al. [66].

Fig. 11.

4. Conclusions

In this work, highly soluble $LiNO_3$ was employed as the neutrally aqueous

electrolyte for the AC-based EDLCs, and the systematical investigations on its physicochemical properties (ionic conductivity and viscosity) and electrochemical characteristics were done in comparison with the most studied Li_2SO_4 aqueous solution. The results reveal that the $LiNO_3$ aqueous solution displays more desirable physicochemical properties and electrochemical performances as the neutral electrolyte for EDLCs. More specifically, the 5.0 M $LiNO_3$ aqueous solution displays a conductivity value up to 154.8 mS cm^{-1} at 25 °C, nearly two times of that for the 2.0 M Li_2SO_4 aqueous solution. The absolute viscosity of the 9.0 M $LiNO_3$ aqueous solution is only 2.4, while that of the 2.5 M Li_2SO_4 aqueous solution achieves 3.0. Both the 5.0 M $LiNO_3$ and 2.0 M Li_2SO_4 aqueous electrolytes hold the operating cell voltages of 1.8 V. The EDLC fabricated with the 5.0 M $LiNO_3$ aqueous electrolyte affords an energy density up to 21.16 Wh Kg^{-1} at a power density of 100.09 W kg^{-1}, substantially higher than 18.43 Wh Kg^{-1} for the EDLC with the 2.0 M Li_2SO_4 aqueous electrolyte at the identical power density. The EDLC with 5.0 M $LiNO_3$ aqueous electrolyte also possesses good cyclic stability. After 10000 charge–discharge cycles at a current density of 1 A g^{-1} and a cut-off voltage of 1.8 V, the capacity retention of the EDLC with 5.0 M $LiNO_3$ aqueous electrolyte retains 90.8%, still higher than 89.4% of the EDLC with the 2.0 M Li_2SO_4 aqueous electrolyte. Therefore, it can be reasonably concluded that the neutral $LiNO_3$ aqueous solution may be a promising candidate electrolyte for the eco-friendly and inexpensive EDLCs.

Acknowledgements

This work was financially supported by National Natural Science Foundation of China (No. 21171174 and 21505035), Provincial Natural Science Foundation of Hunan (No. 2016JJ3028), the opening subject of State Key Laboratory of Powder Metallurgy, and the Hunan Provincial Science and Technology Plan Project (No. 2017TP1001).

References

[1] J.B. Goodenough, Electrochemical energy storage in a sustainable modern society, Energ. Environ. Sci. 7 (2014) 14–18.

[2] L. Zhao, C. Yang, P. Shen, Z. Wang, C. Deng, L. Yang, J. Li, D. Qian, A brand-new strategy for remarkable improvements of electrochemical performances on conducting polymer-based flexible supercapacitors by coating Mo−Ni−P, Electrochim. Acta 249 (2017) 318−327.

[3] C. Deng, L. Yang, C. Yang, P. Shen, L. Zhao, Z. Wang, C. Wang, J. Li, D, Qian, Spinel $FeCo_2S_4$ nanoflower arrays grown on Ni foam as novel binder-free electrodes for long-cycle-life supercapacitors, Appl. Surf. Sci. 428 (2018) 148–153.

[4] J. Liu, D. Qian, H. Feng, J. Li, J. Jiang, S. Peng, Y. Liu, Designed synthesis of TiO_2-modified iron oxides on/among carbon nanotubes as a superior lithium-ion storage material, J. Mater. Chem. A 2 (2014) 11372−11381.

[5] C. Yin, C. Yang, M. Jiang, C. Deng, L. Yang, J. Li, D. Qian, A novel and facile one-pot solvothermal synthesis of PEDOT–PSS/Ni–Mn–Co–O hybrid as an advanced supercapacitor electrode material, ACS Appl. Mater. Interfaces 8 (2016) 2741−2752.

[6] J. Liu, Y. Zhang, Y. Li, J. Li, Z. Chen, H. Feng, J. Li, J. Jiang, D. Qian, In situ chemical synthesis of sandwich-structured MnO_2/graphene nanoflowers and their supercapacitive behavior, Electrochim. Acta 173 (2015) 148−155.

[7] M.A. Hannan, M.M. Hoque, A. Mohamed, A. Ayob, Review of energy storage systems for electric vehicle applications: Issues and challenges, Renewable Sustainable Energy Rev. 69 (2017) 771−789.

[8] Z. Wu, L. Li, J. Yan, X. Zhang, Materials design and system construction for conventional and new-concept supercapacitors, Adv. Sci. 4 (2017) 1600382.

[9] D. Luo, Y. Li, J. Liu, H. Feng, D. Qian, S. Peng, J. Jiang, One-step solution-phase synthesis of a novel RGO–Cu_2O–TiO_2 ternary nanocomposite with excellent cycling stability for supercapacitors, J. Alloy. Compd. 2013, 581, 303−307.

[10] D. Qu, Mechanistic studies for the limitation of carbon supercapacitor voltage, J. Appl. Electrochem. 39 (2009) 867−871.

[11] C. Zhong, Y. Deng, W. Hu, J. Qiao, L. Zhang, J. Zhang, A review of electrolyte materials and compositions for electrochemical supercapacitors, Chem. Soc. Rev. 44 (2015) 7484−7539.

[12] F. Béguin, V. Presser, A. Balducci, E. Frackowiak, Carbons and electrolytes for advanced supercapacitors, Adv. Mater. 26 (2014) 2219−2251.

[13] P. Simon, Y. Gogotsi, Capacitive energy storage in nanostructured carbon–electrolyte systems, Accounts Chem. Res. 46 (2013) 1094−1103.

[14] S. Zhang, J. Sun, X. Zhang, J. Xin, Q. Miao, J. Wang, Ionic liquid-based green processes for energy production, Chem. Soc. Rev. 43 (2014) 7838−7869.

[15] D.R. MacFarlane, N. Tachikawa, M. Forsyth, J.M. Pringle, P.C. Howlett, G.D. Elliott, J.H. Davis, M. Watanabe, P. Simon, C.A. Angell, Energy applications of ionic liquids, Energ. Environ. Sci. 7 (2014) 232−250.

[16] E. Frackowiak, Q. Abbas, F. Béguin, Carbon/carbon supercapacitors, J. Energy Chem. 22 (2013) 226−240.

[17] A. Burke, R&D considerations for the performance and application of

electrochemical capacitors, Electrochim. Acta 53 (2007) 1083−1091.

[18] Y. Wang, Y. Song, Y. Xia, Electrochemical capacitors: mechanism, materials, systems, characterization and applications, Chem. Soc. Rev. 45 (2016) 5925−5950.

[19] E.G. Calvo, N. Ferrera-Lorenzo, J.A. Menéndez, A. Arenillas, Microwave synthesis of micro-mesoporous activated carbon xerogels for high performance supercapacitors, Micropor. Mesopor. Mater. 168 (2013) 206−212.

[20] Y. Zhao, M. Liu, L. Gan, X. Ma, D. Zhu, Z. Xu, L. Chen, Ultramicroporous carbon nanoparticles for the high-performance electrical double-layer capacitor electrode, Energ. Fuel. 28 (2014) 1561−1568.

[21] P. Ratajczak, K. Jurewicz, F. Béguin, Factors contributing to ageing of high voltage carbon/carbon supercapacitors in salt aqueous electrolyte, J. Appl. Electrochem. 44 (2014) 475−480.

[22] G. Ma, D. Guo, K. Sun, H. Peng, Q. Yang, X. Zhou, X. Zhao, Z. Lei, Cotton-based porous activated carbon with a large specific surface area as an electrode material for high-performance supercapacitors, RSC Adv. 5 (2015) 64704−64710.

[23] E.G. Calvo, F. Lufrano, A. Arenillas, A. Brigandì, J.A. Menéndez, P. Staiti, Effect of unequal load of carbon xerogel in electrodes on the electrochemical performance of asymmetric supercapacitors, J. Appl. Electrochem. 44 (2014) 481−489.

[24] D. Jiménez-Cordero, F. Heras, M.A. Gilarranz, E. Raymundo-Piñero, Grape seed carbons for studying the influence of texture on supercapacitor behaviour in aqueous electrolytes, Carbon 71 (2014) 127–138.

[25] K. Fic, G. Lota, M. Meller, E. Frackowiak, Novel insight into neutral medium as electrolyte for high-voltage supercapacitors, Energ. Environ. Sci. 5 (2012) 5842–5850.

[26] J. Jiang, J. Liu, S. Peng, D. Qian, D. Luo, Q. Wang, Z. Tian, Y. Liu, Facile synthesis of α-MoO_3 nanobelts and their pseudocapacitive behavior in an aqueous Li_2SO_4 solution, J. Mater. Chem. A 1 (2013) 2588–2594.

[27] Q. Gao, L. Demarconnay, E. Raymundo-Pinero, F. Béguin, Exploring the large voltage range of carbon/carbon supercapacitors in aqueous lithium sulfate electrolyte, Energ. Environ. Sci. 5 (2012) 9611–9617.

[28] J. Jiang, G. Tan, S. Peng, D. Qian, J. Liu, D. Luo, Y. Liu, Electrochemical performance of carbon-coated $Li_3V_2(PO_4)_3$ as a cathode material for asymmetric hybrid capacitors, Electrochim. Acta 107 (2013) 59–65.

[29] J.H. Chae, G.Z. Chen, 1.9 V aqueous carbon–carbon supercapacitors with unequal electrode capacitances, Electrochim. Acta 86 (2012) 248–254.

[30] A. Seidell, Solubilities of inorganic and organic substances, D. Van Nostrand Company, New York, 1919.

[31] H. Luo, Y. Yang, B. Mu, Y. Chen, J. Zhang, X. Zhao, Facile synthesis of microporous carbon for supercapacitors with a $LiNO_3$ electrolyte, Carbon 100 (2016) 214–222.

[32] I.M. Abdulagatov, A.B. Zeinalova, N.D. Azizov, Viscosity of aqueous $Ni(NO_3)_2$ solutions at temperatures from (297 to 475) K and at pressures up to 30 MPa and concentration between (0.050 and 2.246) mol kg^{-1}, J. Chem. Thermodyn.

Thermochem. 38 (2006) 179−189.

[33] I.M. Abdulagatov, A. Zeinalova, N.D. Azizov, Viscosity of aqueous Na_2SO_4 solutions at temperatures from 298 to 573 K and at pressures up to 40 MPa, Fluid Phase Equilibr. 227 (2005) 57−70.

[34] T. Isono, Density, viscosity, and electrolytic conductivity of concentrated aqueous electrolyte solutions at several temperatures. Alkaline-earth chlorides, lanthanum chloride, sodium chloride, sodium nitrate, sodium bromide, potassium nitrate, potassium bromide, and cadmium nitrate, J. Chem. Eng. Data 29 (1984) 45−52.

[35] M. Kim, I. Oh, J. Kim, Effects of different electrolytes on the electrochemical and dynamic behavior of electric double layer capacitors based on a porous silicon carbide electrode, Phys. Chem. Chem. Phys. 17 (2015) 16367−16374.

[36] Q. Qu, B. Wang, L. Yang, Y. Shi, S. Tian, Y. Wu, Study on electrochemical performance of activated carbon in aqueous Li_2SO_4, Na_2SO_4 and K_2SO_4 electrolytes, Electrochem. Commun. 10 (2008) 1652−1655.

[37] K. Tsay, L. Zhang, J. Zhang, Effects of electrode layer composition/thickness and electrolyte concentration on both specific capacitance and energy density of supercapacitor, Electrochim. Acta 60 (2012) 428−436.

[38] M. Morita, M. Goto, Y. Matsuda, Ethylene carbonate-based organic electrolytes for electric double layer capacitors, J. Appl. Electrochem. 22 (1992) 901−908.

[39] M. Ue, K. Ida, S. Mori, Electrochemical properties of organic liquid electrolytes based on quaternary onium salts for electrical double ‐ layer capacitors, J. Electrochem. Soc. 141 (1994) 2989−2996.

[40] M. Galiński, A. Lewandowski, I. Stępniak, Ionic liquids as electrolytes, Electrochim. Acta 51 (2006) 5567−5580.

[41] T. Morimoto, K. Hiratsuka, Y. Sanada, K. Kurihara, Electric double-layer capacitor using organic electrolyte, J. Power Sources 60 (1996) 239–247.

[42] A. Brandt, S. Pohlmann, A. Varzi, A. Balducci, S. Passerini, Ionic liquids in supercapacitors, MRS Bull. 38 (2013) 554–559.

[43] A. Boisset, L. Athouël, J. Jacquemin, P. Porion, T. Brousse, M. Anouti, Comparative performances of birnessite and cryptomelane MnO_2 as electrode material in neutral aqueous lithium salt for supercapacitor application, J. Phys. Chem. C 117 (2013) 7408–7422.

[44] J. Kielland, Individual activity coefficients of ions in aqueous solutions, J. Am. Chem. Soc. 59 (1937) 1675−1678.

[45] M. Arulepp, L. Permann, J. Leis, A. Perkson, K. Rumma, A. Jänes, E. Lust, Influence of the solvent properties on the characteristics of a double layer capacitor, J. Power Sources 133 (2004) 320−328.

[46] E. Redondo, E. Goikolea,R. Mysyk, The decisive role of electrolyte concentration in the performance of aqueous chloride-based carbon/carbon supercapacitors with extended voltage window, Electrochim. Acta 221 (2016) 177−183.

[47] J.H. Chae, G.Z. Chen, Influences of ions and temperature on performance of carbon nano-particulates in supercapacitors with neutral aqueous electrolytes, Particuology 15 (2014) 9−17.

[48] X. Sun, X. Zhang, H. Zhang, D. Zhang, Y. Ma, A comparative study of activated carbon-based symmetric supercapacitors in Li_2SO_4 and KOH aqueous electrolytes, J. Solid State Electrochem. 16 (2012) 2597−2603.

[49] H.D. Yoo, J.H. Jang, J.H. Ryu, Y. Park, S.M. Oh, Impedance analysis of porous carbon electrodes to predict rate capability of electric double-layer capacitors, J. Power Sources 267 (2014) 411−420.

[50] R. Kötz, M. Carlen, Principles and applications of electrochemical capacitors, Electrochim. Acta 45 (2000) 2483−2498.

[51] A. Laheäär, A. Jänes, E. Lust, Electrochemical properties of carbide-derived carbon electrodes in non-aqueous electrolytes based on different Li-salts, Electrochim. Acta 56 (2011) 9048–9055.

[52] T. Thomberg, A. Jänes, E. Lust, Energy and power performance of vanadium carbide derived carbon electrode materials for supercapacitors, J. Electroanal. Chem. 630 (2009) 55–62.

[53] M. Taleb, J. Nerut, T. Tooming, T. Thomberg, E. Lust, Oxygen electroreduction on platinum nanoparticles activated electrodes deposited onto D-glucose derived carbon support in 0.1 M KOH, J. Electrochem. Soc. 163 (2016) F1251–F1257.

[54] M.E. Orazem, N. Pébère, B. Tribollet, Enhanced graphical representation of electrochemical impedance data, J. Electrochem. Soc. 153 (2006) B129–B136.

[55] M. Taleb, J. Nerut, T. Tooming, T. Thomberg, A. Jänes, E. Lust, Oxygen electroreduction on platinum nanoparticles deposited onto D-glucose derived carbon, J. Electrochem. Soc. 162 (2015) F651–F660.

[56] X. Zhang, X. Wang, L. Jiang, H. Wu, C. Wu, J. Su, Effect of aqueous electrolytes on the electrochemical behaviors of supercapacitors based on hierarchically porous carbons, J. Power Sources 216 (2012) 290–296.

[57] K. Xu, M.S. Ding, T. Richard Jow, A better quantification of electrochemical stability limits for electrolytes in double layer capacitors, Electrochim. Acta 46 (2001) 1823–1827.

[58] C. Wessells, R. Ruffo, R.A. Huggins, Y. Cui, Investigations of the electrochemical stability of aqueous electrolytes for lithium battery applications, Electrochem. Solid-State Lett. 13 (2010) A59–A61.

[59] K. Xu, S.P. Ding, T.R. Jow, Toward reliable values of electrochemical stability limits for electrolytes, J. Electrochem. Soc. 146 (1999) 4172–4178.

[60] D. Weingarth, H. Noh, A. Foelske-Schmitz, A. Wokaun, R. Kötz, A reliable determination method of stability limits for electrochemical double layer capacitors, Electrochim. Acta 103 (2013) 119–124.

[61] L. Dagousset, G. Pognon, G.T.M. Nguyen, F. Vidal, S. Jus, P. Aubert, Electrochemical characterisations and ageing of ionic liquid/γ-butyrolactone mixtures as electrolytes for supercapacitor applications over a wide temperature range, J. Power Sources 359 (2017) 242–249.

[62] A. Laheäär, P. Przygocki, Q. Abbas, F. Béguin, Appropriate methods for evaluating the efficiency and capacitive behavior of different types of supercapacitors, Electrochem. Commun. 60 (2015) 21–25.

[63] J.P. Zheng, P.C. Goonetilleke, C.M. Pettit, D. Roy, Probing the electrochemical

double layer of an ionic liquid using voltammetry and impedance spectroscopy: A comparative study of carbon nanotube and glassy carbon electrodes in $[EMIM]^+[EtSO_4]^-$, Talanta 81 (2010) 1045–1055.

[64] J.P. Zheng, C.M. Pettit, P.C. Goonetilleke, G.M. Zenger, D. Roy, D.C. voltammetry of ionic liquid-based capacitors: Effects of Faradaic reactions, electrolyte resistance and voltage scan speed investigated using an electrode of carbon nanotubes in EMIM-$EtSO_4$, Talanta 78 (2009) 1056–1062.

[65] L. Eliad, G. Salitra, A. Soffer, D. Aurbach, Ion sieving effects in the electrical double layer of porous carbon electrodes: Estimating effective ion size in electrolytic solutions, J. Phys. Chem. B 105 (2001) 6880–6887.

[66] H.A. Mosqueda, O. Crosnier, L. Athouël, Y. Dandeville, Y. Scudeller, P. Guillemet, D.M. Schleich, T. Brousse, Electrolytes for hybrid carbon-MnO_2 electrochemical capacitors, Electrochim. Acta 55 (2010) 7479−7483.

Figure captions

Fig. 1. Ionic conductivities and viscosities of Li_2SO_4 and $LiNO_3$ aqueous solutions as a function of the molar concentrations measured at 25 °C.

Fig. 2. Nyquist plots of the EDLC cells with 2 M Li_2SO_4 (red) and 5 M $LiNO_3$ (black) aqueous electrolytes: (a) full views and (b) enlarged views of (a) with different axis scales.

Fig. 3. (a) Dependences of the series capacitance (*C*s) and parallel capacitance (*C*p) on log(*f*) at *E* = 0.1 V, and (b) dependences of log /–Z``/ on log(*f*) at *E* = 0.1 V.

Fig. 4. Dependence of capacitances on frequencies for the cells with 2 M Li_2SO_4 and 5 M $LiNO_3$ aqueous electrolytes.

Fig. 5. ESPWs for the 2.0 M Li_2SO_4 and 5.0 M $LiNO_3$ aqueous electrolytes on the Pt electrode at 25 °C.

Fig. 6. CV curves of the (a) 2.0 M Li_2SO_4 and (b) 5.0 M $LiNO_3$ aqueous electrolytes on the AC electrode, and the corresponding plots of evolution of R factor vs. the vertex potential for the (c) 2.0 M Li_2SO_4 and 5.0 M $LiNO_3$ aqueous electrolytes at a scan rate of 5 mV s^{-1} and 25 °C.

Fig. 7. Charge−discharge curves of AC-based EDLCs with the 2.0 M Li_2SO_4 (a) and 5.0 M $LiNO_3$ (b) aqueous electrolytes at 500 mA g^{-1} from 1.2 to 2.0 V.

Fig. 8. CV curves of EDLCs with the (a) 2.0 M Li_2SO_4 and (b) 5.0 M $LiNO_3$ aqueous electrolytes with the current response expressed as the specific capacitance in the voltage range of 0−1.8 V at diverse voltage sweep rates.

Fig. 9. Dependence of specific capacitance retentions of EDLCs with the 2.0 M

Li_2SO_4 (■) and 5.0 M $LiNO_3$ (▲) aqueous electrolytes on the sweep rates.

Fig. 10. Ragone plots of the cells with the 2.0 M Li_2SO_4 (●) and 5.0 M $LiNO_3$ (■) aqueous electrolytes.

Fig. 11. Evolution of the specific discharge capacitance and coulombic efficiency vs. the cycle number for EDLCs with the (a) 2.0 M Li_2SO_4 and (b) 5.0 M $LiNO_3$ aqueous electrolytes at a current density of 1 A g^{-1} and a cut-off voltage of 1.8 V.

Table caption

Table 1 Comparisons of columbic efficiency (η_t) and energy efficiency (η_E) of cells with 2.0 M Li_2SO_4 and 5.0 M $LiNO_3$ at different cell potentials.

Table 1

Comparisons of columbic efficiency (η_t) and energy efficiency (η_E) of cells with 2.0 M Li_2SO_4 and 5.0 M $LiNO_3$ at different cell potentials.

Cell voltage/V	2.0 M Li_2SO_4		5.0 M $LiNO_3$	
	η_t /%	η_E /%	η_t /%	η_E /%
1.2	99.95	79.11	99.55	88.72
1.4	99.83	78.24	99.23	87.09
1.6	98.51	77.07	98.34	84.87
1.8	96.84	74.27	97.41	81.82
2.0	94.27	69.25	92.84	72.59

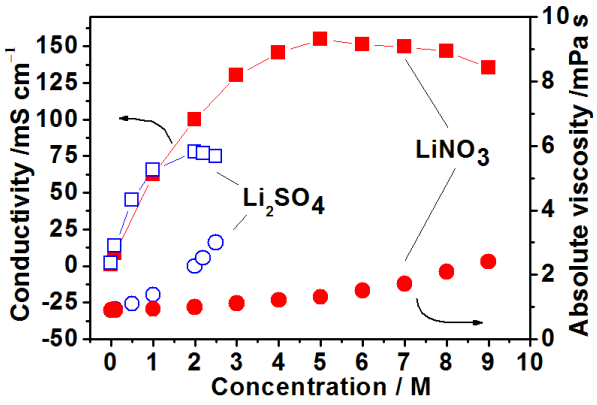

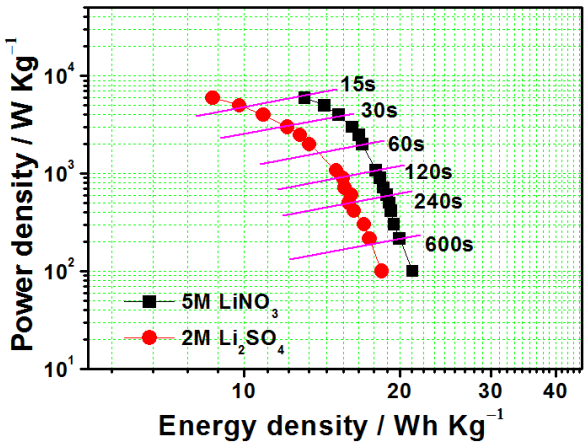

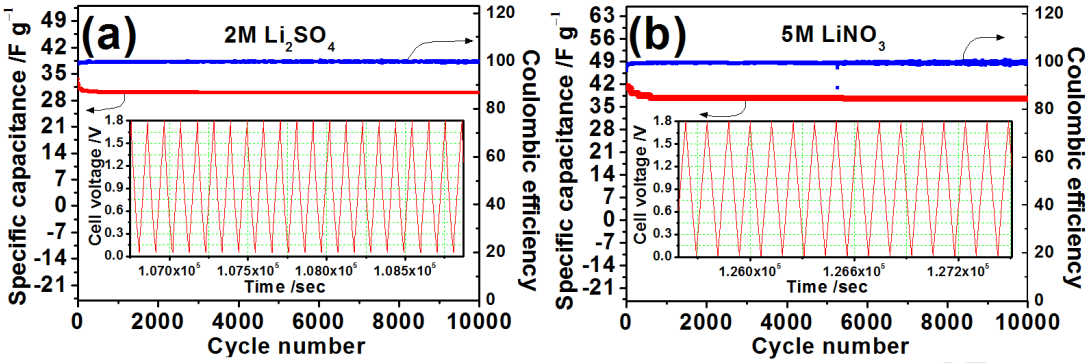

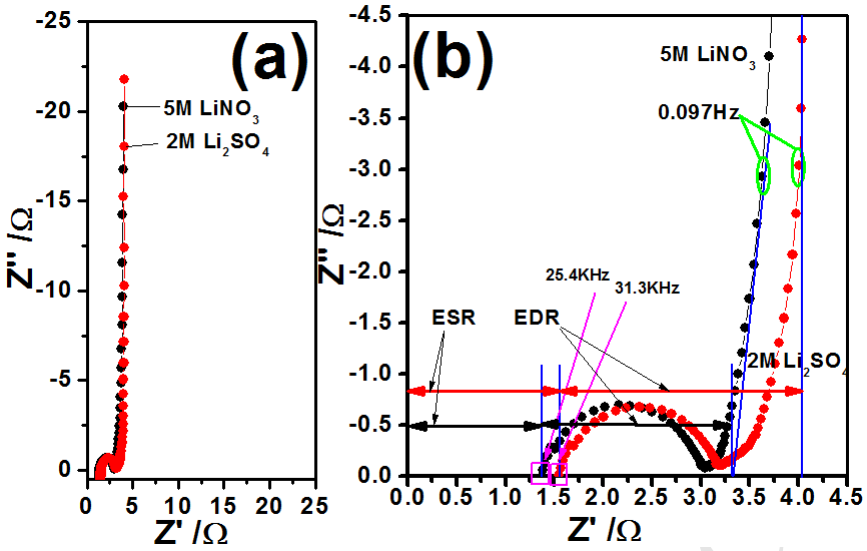

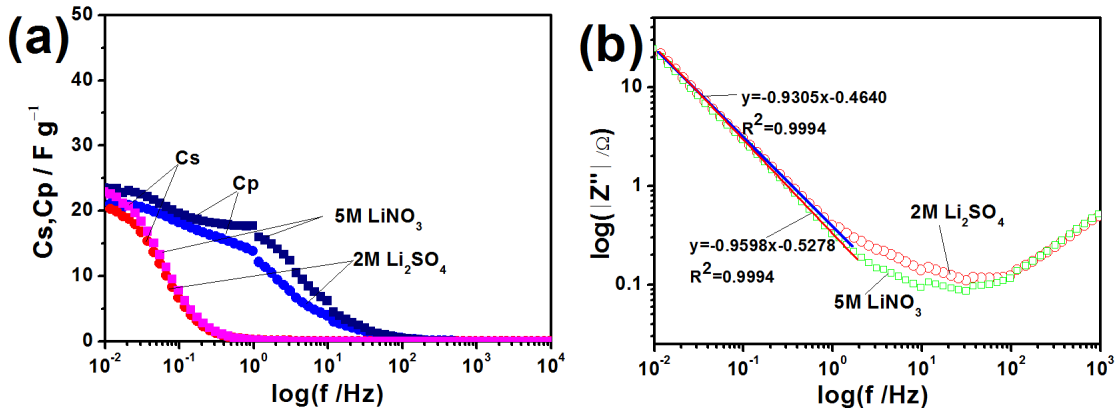

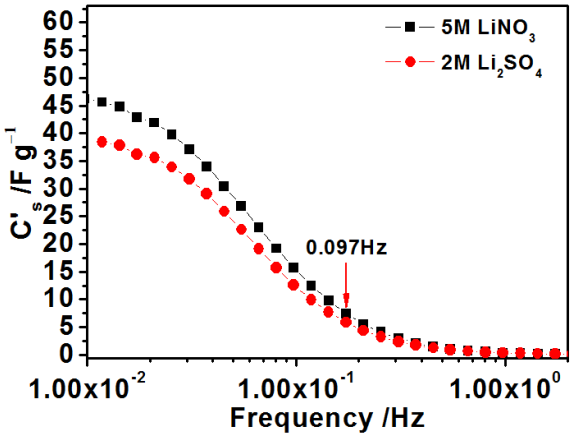

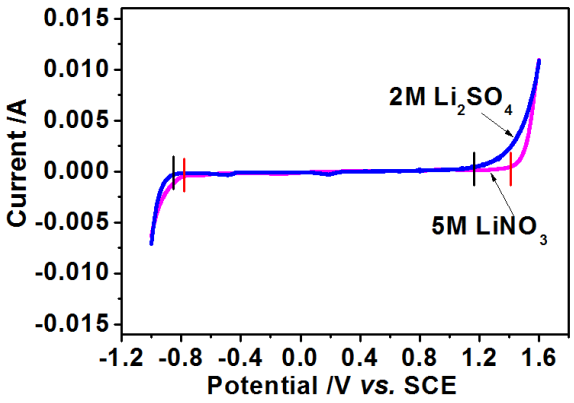

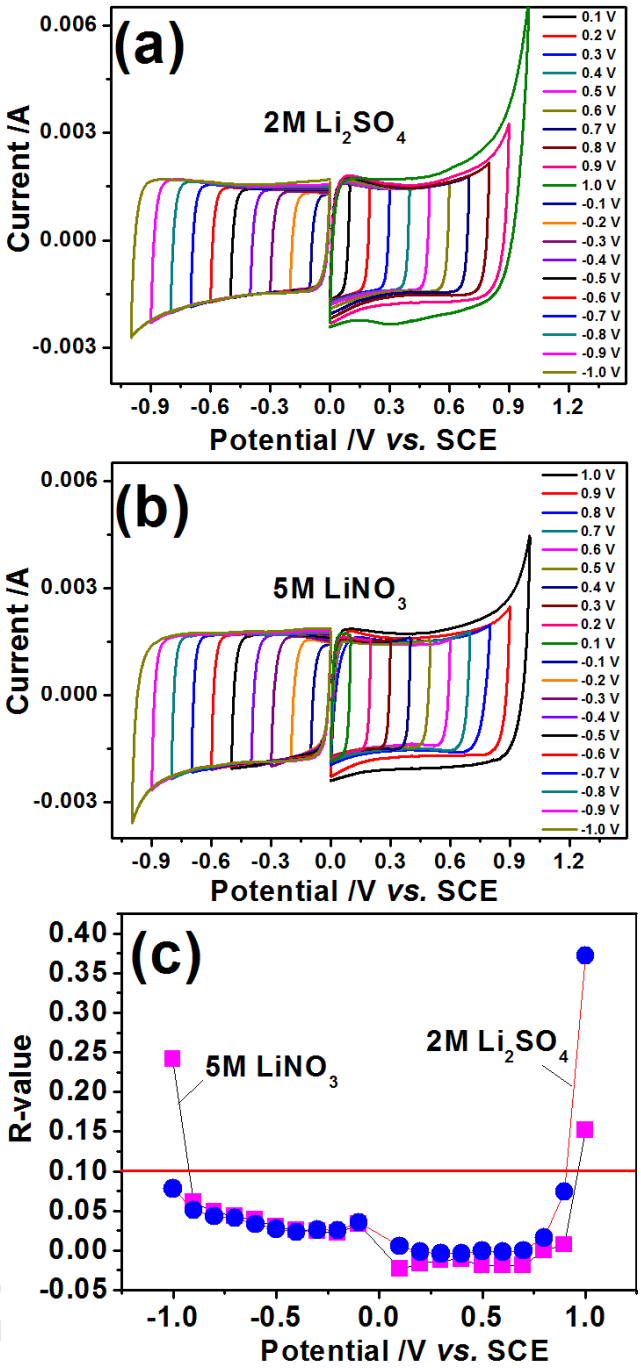
(a)
2M Li2SO4
Current /A
Potential /V vs. SCE
0.1 V
0.2 V
0.3 V
0.4 V
0.5 V
0.6 V
0.7 V
0.8 V
0.9 V
1.0 V
-0.1 V
-0.2 V
-0.3 V
-0.4 V
-0.5 V
-0.6 V
-0.7 V
-0.8 V
-0.9 V
-1.0 V
(b)
5M LiNO3
Current /A
Potential /V vs. SCE
1.0 V
0.9 V
0.8 V
0.7 V
0.6 V
0.5 V
0.4 V
0.3 V
0.2 V
0.1 V
-0.1 V
-0.2 V
-0.3 V
-0.4 V
-0.5 V
-0.6 V
-0.7 V
-0.8 V
-0.9 V
-1.0 V
(c)
5M LiNO3
2M Li2SO4
R-value
Potential /V vs. SCE